TISSUE ENGINEERING: Part A
Volume 18, Numbers 7 and 8, 2012

DOI: 10.1089/ten.tea.2011.0017

Hypoxic Culture and Insulin Yield Improvements to Fibrin-Based Engineered Tissue

Jason W. Bjork, Ph.D.,[1] Lee A. Meier, B.S.,[1] Sandra L. Johnson, B.S.,[1]
Zeeshan H. Syedain, Ph.D.,[1] and Robert T. Tranquillo, Ph.D.[1,2]

We examined the effect of insulin supplementation and hypoxic culture (2% vs. 20% oxygen tension) on collagen deposition and mechanical properties of fibrin-based tubular tissue constructs seeded with neonatal human dermal fibroblasts. The results presented here demonstrate that constructs cultured under hypoxic conditions with insulin supplementation increased in collagen density by approximately five-fold and both the ultimate tensile strength (UTS) and modulus by more than three-fold compared with normoxic (20% oxygen tension), noninsulin supplemented controls. In addition, collagen deposited on a per-cell basis increased by approximately four-fold. Interaction was demonstrated for hypoxia and insulin in combination in terms of UTS and collagen production on a per-cell basis. This interaction resulted from two distinct processes involved in collagen fibril formation. Western blot analysis showed that insulin supplementation alone increased Akt phosphorylation and the combined treatment increased collagen prolyl-4-hydroxylase. These molecules are distinct regulators of collagen deposition, having an impact at both the transcriptional and posttranslational modification stages of collagen fibril formation that, in turn, increase collagen density in the tissue constructs. These findings highlight the potential of utilizing insulin supplementation and hypoxic culture in combination to increase the mechanical strength and stiffness of fibrin-based engineered tissues.

Introduction

Statistics from the American Heart Association show that over 448,000 coronary artery bypass graft (CABG) procedures were performed in 2006.[1] Autologous blood vessels are often used for CABG surgery but they are not always available due to previous harvest, anatomical limitations, or disease progression. The field of cardiovascular tissue engineering has attempted to produce a clinically viable synthetic conduit by using a variety of *in vitro* approaches that combine living cells either seeded on a synthetic biodegradable polymer or into a biopolymer-based scaffold.[2] Synthetic scaffolds are chosen for mechanical strength, range of processing methods, and ability to tailor properties such as the degree of cross-linking; however, synthetic materials often induce gradients of potentially detrimental degradation products. In contrast, biopolymer-based scaffolds allow the potential for a completely biological vascular conduit, but do not always achieve the degree of mechanical strength required for *in vivo* use.[3,4]

A fibrin scaffold, in particular, possesses several advantages over alternative approaches. Cell-induced fiber alignment during *in vitro* tissue development,[5,6] enhanced cell-binding properties,[7] collagen synthesis,[6,8] and the ability to be remodeled via intrinsic cellular enzymatic processes[9] present motivation for utilizing fibrin as the scaffold. However, fibrin has been only able to achieve adequate strengths required for reliable use *in vivo* in conjunction with advanced bioreactors.[10–12] Enhancing the production of extracellular matrix (ECM) components, primarily collagen, is necessary to increase the mechanical strength of fibrin-based engineered tissues. Previous research in our lab with such tissues has shown the ability of insulin supplementation to enhance collagen production.[8,13] More recently, Balguid *et al.* have demonstrated the advantage of culturing in a 7% O_2 environment with and without insulin supplementation to increase collagen density and mechanical properties in model tissues where fibrin was used in conjunction with a synthetic polymer scaffold.[14]

Though most *in vitro* cell and tissue culture experimentation is conducted near atmospheric oxygen concentrations (pO_2 typically 20% which equals a concentration of dissolved oxygen (DO) = 193 nmol/mL), an environment that presents cells with a low O_2 tension is more physiologically relevant. *In vivo*, the oxygen concentration of inspired air falls below atmospheric levels due to increased temperature and humidification before reaching the blood stream. Aortic oxygen levels have been found to be ~110 nmol/mL at the lumenal

Departments of [1]Biomedical Engineering and [2]Chemical Engineering and Materials Science, University of Minnesota, Minneapolis, Minnesota.

surface and fall to 20 nmol/mL at distances of 150 μm into the tissue.[15,16] Other tissues, such as articular cartilage can reach lower levels of DO without being damaged.[17] Dermal wound healing responses have also been described as hypoxic environments,[18,19] leading to increased collagen deposition and fibrosis.

There is conflicting evidence, however, regarding the effects of hypoxia on cells both *in vitro* and *in vivo*, as the effects of low O_2 typically vary depending on the cell type or species in question.[20] For example, chondrocytes benefit from low oxygen tension (2%) to help maintain a glycolytic versus an oxidative phenotype[21] but have higher proliferation rates with increased oxygen tensions.[22] Ocular cells also have been shown to have varied metabolism in low oxygen environments.[23] In contrast, smooth muscle cells have shown varied results. Ray *et al.* demonstrated increased proliferation at an oxygen tension of 3%, but greater levels of apoptosis at 1%, suggesting a balance between hypoxic and severely hypoxic pO_2 levels for this cell type.[15] Dermal fibroblasts, the focus of this study, have demonstrated increased collagen deposition and increased secretion of a range of collagen production-inducing growth factors when cultured in environments with oxygen tensions at or below 2%.[18,24]

In this study, we evaluated collagen production and mechanical properties of fibrin-based tubular tissue constructs cultured in an environment with low oxygen tension (2% pO_2). Preliminary investigations conducted at 5% pO_2 showed no substantial increases in mechanical properties and collagen deposition; thus, experimentation was conducted using 2% pO_2, similar to work conducted by Falanga *et al.*,[18] which demonstrated increased collagen content with hDFs cultured at this pO_2. In addition, previous work in our lab,[6,8,25] demonstrated the benefits of insulin supplementation at 2 μg/mL on collagen deposition and increased mechanical strength and stiffness. The effects of 2% pO_2 and insulin supplementation were further investigated by Western blot analysis of key regulators of collagen fibril production to gain insight into changes in signaling and collagen posttranslational processing. Specifically, Akt,[26] extracellular signal-regulated kinase (ERK),[10,27] and collagen prolyl-4-hydroxylase (P4H)[24] were investigated. A mathematical analysis of the predicted DO profile in the tissue was also performed to evaluate the possibility of anoxic conditions (0% pO_2) in constructs statically cultured versus continuously mixed in presumed hypoxic conditions.

Materials and Methods

Cell culture

Neonatal human dermal fibroblasts (nhDFs; Clonetics) were maintained in 50:50 Dulbecco's modified Eagle Medium (DMEM)/F12 (Invitrogen) containing 15% fetal bovine serum (FBS) and 100 U/mL penicillin, 100 μg/mL streptomycin (Invitrogen) on tissue culture plastic in a 5% CO_2, 37°C, humidified incubator. Cells were passaged at confluency and harvested for use at passage 9.

Tissue construct preparation and culture

Fibrin-based tubular constructs were prepared as previously described.[8] Briefly, bovine fibrinogen (Sigma), cells, and thrombin (Sigma) were mixed in a 4:1:1 ratio to achieve a final concentration of 3 mg/mL fibrin and 0.5×10^6 cells/mL. This mixture was then injected into a tubular mold housing a 2 mm glass mandrel pretreated with Pluronic F-127 (Sigma) to minimize gel adhesion. Gels were allowed to vertically form for 30 min before mold removal and transferred into a 15 cm culture dish. Culture medium consisted of DMEM (Gibco) supplemented with 10% FBS (Hyclone), 50 μg/mL L-ascorbic acid, 100 U/mL penicillin, 100 μg/mL streptomycin, and 0.25 μg/mL amphotericin-B. Insulin was absent or supplemented at 2 μg/mL (the insulin concentration in the FBS reported by the supplier is ~300 pg/mL).

Fibrin gel hemispheres were employed for protein analysis by Western blot. The hemispheres were formed using a similar solution as described above except the solution was cast into circular scores made in each well of 12-well plates, similar to the method used by Tuan and Grinnell.[28] The same medium as that employed for culturing tubular constructs was used for hemisphere culture. After casting, both tubular and hemisphere constructs were maintained in a standard 5% CO_2 incubator for the first 24 h to allow for initial gel compaction. After this initial incubation period, constructs were either maintained in a standard 5% CO_2 incubator or moved to a nitrogen-purged incubator with a pO_2 set point of 2%.

While care was taken to minimize the exposure time to ambient oxygen conditions, the hypoxic culture treatment group was briefly subjected to oxygen concentrations above the 2% pO_2 setpoint when the culture medium was replaced. At a frequency of three times per week, this treatment group experienced a pO_2 increase from 2% up to ambient levels, then back down to 2% over the course of ~1 h.

Measurement of oxygen consumption rate

Oxygen consumption rate (OCR) was measured for cultured nhDFs using a stirred microchamber and an oxygen-monitoring system as previously described.[29,30] The microchamber (Instech Labs, Inc.) consisted of a water-jacketed titanium cup sealed with a glass plug. A fluorescence-based oxygen sensor was mounted inside, which was linked via fiber optics to a fluorescence lifetime instrument (Presens Precision Sensing, GmbH). The system monitored oxygen concentration in the medium at 1 s intervals over the course of the tests. These data were exported to MATLAB to extract the sample OCR and Michaelis–Menten kinetic parameters as previously described.[29] Measurements taken using this system provided changes in DO due to metabolic oxygen consumption inside the chamber. OCR was obtained on a per-cell basis after quantification of the number of cells and qualitative assessment of viability by trypan blue staining.

Mathematical model for DO transport and parameters

DO profiles were predicted using the finite element method software package COMSOL Multiphysics (version 3.5; COMSOL, Inc.), which accounted for nonlinear (Michaelis–Menten) consumption kinetics and DO diffusion.[29,31,32] The model was idealized using an axisymmetric domain for a tubular construct incubated on a solid mandrel of infinite length as previously described.[29] The model was used to predict oxygen gradients in static culture by setting the incubator pO_2 as a boundary condition at the air-culture medium interface with flux continuity at the culture medium-tissue interface and no flux at all other boundaries. For the mixed cases, the problem was simplified by

effectively enforcing the incubator pO_2 as the boundary condition at the ablumenal surface of the tissue, thus assuming that the system was perfectly mixed. The cell density was assumed to be uniform throughout the tissue. Additional detail regarding the model and boundary conditions is provided in the Appendix. The model was solved using the UMFPACK stationary solver with a convergence tolerance of 10^{-6} and a minimum damping factor of 10^{-4}.

Uniaxial tensile testing

Dimensions of tissue rings were measured before mechanical loading. Widths and lengths were determined with digital calipers (Mitutoyo). Thicknesses were measured using a 50-g force probe attached to a displacement transducer. The rings were placed onto a T-bar apparatus that was submerged in PBS and uniaxially stretched using a Microbionix Testing System (MTS Systems) to obtain circumferential tensile mechanical properties. Rings were straightened with a 5 mN load to serve as the reference length. Mechanical testing was conducted with six cycles of 0%–10% strain preconditioning followed by stretch to failure at 2 mm/min. True strain was calculated based on the change in length of the rings during the test, whereas engineering stress was calculated as measured force divided by initial cross-sectional area. The modulus was determined by linear-regression of a portion of the stress-strain curve taken from after the toe region to the point of tissue failure. Samples were also mechanically tested in a similar fashion subsequent to a 30-min incubation in 0.05% sodium azide in Hank's buffer solution with an inhibitor cocktail of 10 mM EDTA, 2 μg/mL pepstatin and 1 μg/mL aprotinin, to kill cells within the construct, which allowed measurement of mechanical properties with minimal influence by cellular traction forces.

Protein and cell quantification

A modified ninhydrin-based assay was used to quantify total protein.[33] Collagen content was determined by measuring 4-hydroxyproline, assuming 7.46 g of collagen per gram of 4-hydroxyproline.[34] Construct cellularity was determined using a modified Hoechst assay for DNA, assuming 7.6 pg DNA per cell.[35] Reported collagen and cell density values are on a per-volume of tissue basis. Dimensions of the tissue were obtained as listed for mechanical testing. For cell viability assessment after azide treatment, constructs (control and treated) were immersed in PBS and incubated in DMEM with 2 μM Calcein AM and 4 μM Ethidium homodimer-1 (Invitrogen) for 30 min. The constructs were immersed in PBS for 5 min and then imaged using epi-fluorescence (Olympus IX70) with a 10× objective and excitation and emission wavelengths according to the manufacturer's standard protocol. Multiple fields were imaged and cell counts were used to evaluate percentage of live cells.

Western blots

Western blots were utilized to probe cellular pathways involved in collagen deposition, namely phosphatidylinositol-3-kinase/Akt (PI3K/Akt), ERK, and P4H. Relative amounts of phosphorylated and total Akt (pAkt and tAkt, respectively), phosphorylated and total ERK (pERK and tERK, respectively), and P4H were determined.

All chemicals were obtained from Sigma-Aldrich unless noted otherwise. Hemisphere samples were lysed using sonication in buffer containing 25 mM Tris, 225 mM NaCl, 25 mM NaF, 5% glycerol, 0.5% NP-40, 1 mM EDTA. Halt™ protease and phosphatase inhibitor cocktail (Pierce) was added. For each sample, 20 μg of whole cell lysate were boiled in reducing sample buffer and separated by SDS/PAGE using a 4%–20% acrylamide gradient gel (Bio-Rad Laboratories) with Tris/Glycine running buffer. Two samples from each treatment group were run in parallel. Following gel separation, proteins were transferred to nitrocellulose membranes (Whatman) using wet transfer buffer (10% methanol, 2.2 g/L 3-(cyclohexylamino)-1-propanesulfonic acid, pH11). Blots were incubated in blocking solution (Superblock, Pierce, and 0.1% Tween-20) for 1 h and then incubated with primary antibody overnight at 4°C. Blots were then incubated with species-matched horseradish peroxidase-conjugated secondary antibodies (Jackson) and developed using electrochemiluminescence. Antibodies were removed using stripping buffer (Pierce) and membranes were reprobed for additional molecules. The pERK to tERK and pAkt to tAkt ratios was determined by densitometry of scanned autoradiograms using ImageJ (NIH). Relative comparisons of levels of P4H within different treatment groups were made through normalization to β-actin. Anti-ERK and anti-Akt antibodies were purchased from Cell Signaling Technologies, anti-P4H was purchased from Abcam, and anti-β-actin was obtained from Sigma-Aldrich.

Pyridinium cross-link quantification

Pyridinium cross-links, pyridinoline (PYD) and deoxypyridinoline cross-links were measured using an enzyme immunoassay (EIA) kit, MicroVue PYD EIA (Quidel Corporation). Samples were hydrolyzed for 22–24 h at 110°C in 6 N HCl containing a solubilizing agent (Quidel). Following hydrolysis, the samples were dried in a SpeedVac (Savant), then dissolved in the EIA Assay Buffer to 200 μg/mL or less total protein, and the pH adjusted to 7–8 with NaOH. The samples were then used in the EIA following the manufacture's standard protocol.

Histology

Constructs were fixed with 4% paraformaldehyde for 3 h, rinsed, infiltrated overnight with a solution of 30% sucrose, 5% dimethyl sulfoxide (DMSO) in phosphate buffered saline (PBS), and frozen in OCT. The tissue was then sectioned into 9 μm sections and stained using Lillie's trichrome. After staining, images were taken with 10× or 20× objectives with transmitted light.

Statistical analysis

Reported results were obtained from duplicate or triplicate experiments as noted in figure captions, depending on the response variable measured. All data are presented as mean ± SEM with sample size denoted in figure captions. Statistical significance was determined by one-way analysis of variance (ANOVA) or general linear model ANOVA. Significance versus a control treatment (20% oxygen without insulin supplementation) was conducted with a Dunnett's comparison test. Significance of treatments was conducted using a Bonferroni comparison test. Two-way ANOVA was

also conducted on P4H Western blot densitometry data to evaluate significance of the interaction between insulin supplementation and hypoxic culture. All statistical analyses were conducted using Minitab 15 and a calculated *p*-value of 0.05 or less was considered significant.

Results

Michaelis–Menten parameters determined for nhDF

Data from the stirred microchamber and oxygen monitoring system were used to calculate the Michaelis–Menten parameters for nhDFs. Samples consisted of $\sim 1 \times 10^6$ cells in 150 μL. $V_{max} = 1.66 \pm 0.05$ fmol/min/cell (mean ± standard deviation) and $K_m = 15.8 \pm 2.1$ nmol/mL were determined from O_2 consumption rate curves.

Mathematical analysis of hypoxic culture conditions

The predicted DO profile across the tissue was calculated to understand concentration gradients and to determine the minimum DO in the tissue for different possible experimental configurations. Figure 1 shows the model parameters and resulting DO profile through the thickness of the tissue when cultured in 2% versus 20% pO_2 and for well mixed versus static culture. For the cell densities measured in these experiments, mixed versus static culture did not impact the OCR when cultured in 20% pO_2, as evidenced by the parallel lines (open circles and open triangles) in Figure 1C. Culturing in 2% pO_2, however, resulted in a flattened DO profile due to a decreased consumption rate since DO was less than K_m. The mixed culture had a peak DO of 19.3 nmol/mL at the ablumenal surface (R_o) and decreased to ~2 nmol/mL at the lumenal surface (R_i). The static culture had a similar flattened profile; however, the maximum DO at R_o was similar to the minimum of the mixed culture at 2 nmol/mL and further decreased to 0.1 nmol/mL at R_i.

Uniaxial tensile testing

Figure 2A, B shows the results of insulin supplementation and hypoxic culture on tensile mechanical properties after 5 weeks of culture. Considering the 20% pO_2, noninsulin supplemented group as the control group, increased UTS was observed for all treatment groups and the modulus increased under hypoxic conditions. A 6.2-fold increase in UTS and a 4.8-fold increase in modulus occurred in the hypoxic group with insulin compared with controls. These data, collected over three independent experiments, demonstrate that culture in 2% pO_2 can increase both the strength and stiffness of fibrin-based tissue constructs.

Constructs were tested to examine the cellular contribution to mechanical strength and stiffness (Fig. 2C, D).

A

Variable	Description	Value	
$R_o - R_i$	Tissue thickness	200	μm
ρ_{cell}	Cell density	100 - 200 × 10^6	cell/mL
$Vo_{2,\,max}$	Michaelis-Menten parameter	1.66	fmol · min^{-1} · $cell^{-1}$
K_m	Michaelis-Menten parameter	15.8	nmol/mL
D_t	Effective O_2 diffusivity in tissue	1.06 × 10^{-5}	cm^2/s
D_m	Effective O_2 diffusivity in medium	3.83 × 10^{-5}	cm^2/s
P_∞	O_2 % air saturation (gas phase)	2-20	% air-sat.

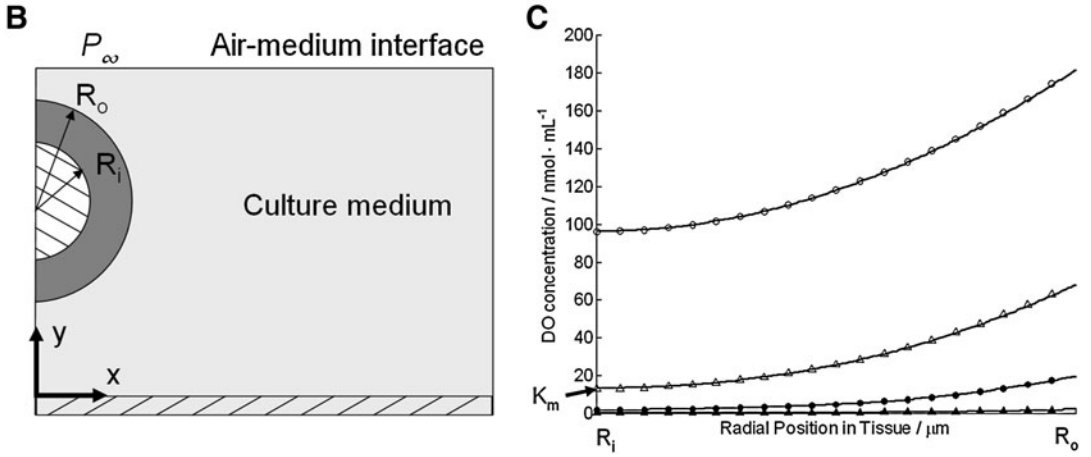

FIG. 1. Mathematical model for DO transport. **(A)** Model parameters used to estimate the DO profile through the tissue for mixed and static cases and 20% versus 2% pO_2. **(B)** Schematic of model system (not to scale). **(C)** Predicted DO profiles through the tissue from the lumenal surface (R_i) to the ablumenal surface (R_o). Closed circles = mixed, 2% pO_2. Open circles = mixed, 20% pO_2. Closed triangles = static culture, 2% pO_2. Open triangles = static culture, 20% pO_2. DO, dissolved oxygen.

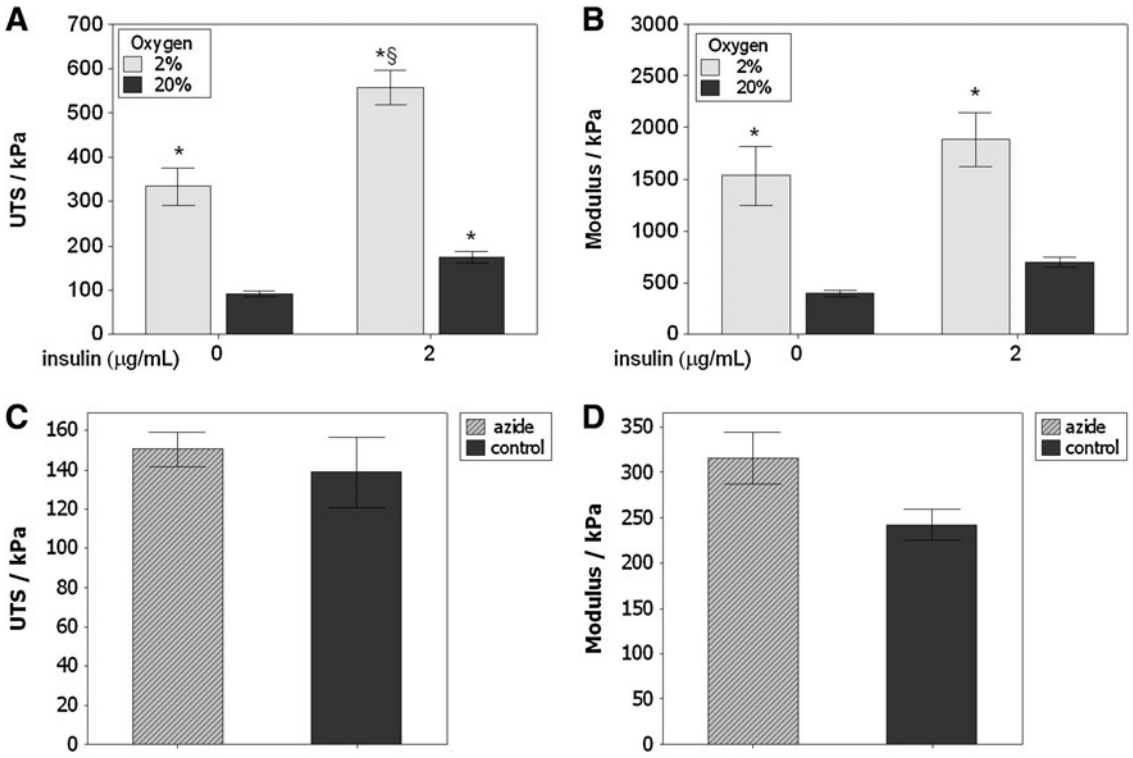

FIG. 2. Uniaxial tensile test results for tissue constructs after 5 weeks of culture. **(A)** Ultimate tensile strength (UTS). Both hypoxic culture (2% pO_2) and insulin supplementation (2 μg/mL) alone yielded an increase in UTS. Hypoxia and insulin together yielded a substantially higher UTS compared with all other groups. **(B)** Modulus. The modulus increased only under hypoxic conditions. $n=12$ for each bar (three independent experiments). The effect of insulin on modulus was marginally significant ($p=0.08$). **(C)** UTS and **(D)** Modulus for tissue cultured under 20% O_2 with insulin, treated with (hatched bars) and without (solid bars) sodium azide to kill the cells in the construct, indicating no contribution of live cells to the mechanical properties of the tissue. *$p<0.05$ compared with control (20% pO_2, no insulin group). §$p<0.05$ compared with all other groups.

Comparison was made between untreated and azide treated samples, both incubated with insulin at 20% oxygen. Control samples had more than 90% live cells (94%±13%), while azide treatment reduced this level to less than 10% (7%±2%), with extensive vacuole formation and loss of typical elongated cell morphology. No difference was observed in UTS or modulus.

Table 1 summarizes the fold-increase calculated from the ANOVA main effects due to insulin and oxygen tension. Evaluation of the means shows that for UTS, a 1.7-fold increase was observed due to insulin and a 3.4-fold increase was observed due to hypoxia. A 6.2-fold increase was observed when comparing the combined hypoxia and insulin treatment to the control group (20% pO_2 without insulin). The ANOVA indicates an interaction between hypoxia and insulin for UTS. A 3.2-fold increase was observed in the modulus due to hypoxia; there was no increase due to insulin.

Cell, collagen, and pyridinium density quantification

Cell density and collagen density both increased for constructs cultured in a hypoxic environment. Figure 3 shows over a two-fold increase in cell density and nearly a four-fold increase in collagen density for tissues cultured in 2% pO_2 versus 20% pO_2 (final tissue volumes at harvest were comparable among all groups (data not shown)). Evaluation of the amount of deposited collagen per cell revealed an increase for the insulin treated samples, and the combination of 2% pO_2 with insulin yielded more collagen per cell versus 20% pO_2 and insulin. Thus, it is likely that the collagen density for the hypoxia treatment alone was higher due to the higher cell density. As highlighted in Table 1, the interaction term was statistically significant according to the ANOVA.

Table 1. ANOVA Main Effects Summary (With Propagated Error). The Fold-Increase Was Determined with Treatment Means from a Two-Way ANOVA

	Fold-increase summary		
Treatment	*UTS (kPa)*	*E (kPa)*	*Collagen/cell (pg)*
Insulin	1.7±0.2[a]	1.4±0.2	2.7±0.5[a]
2% O_2	3.4±0.6[a]	3.2±0.8[a]	1.8±0.4[a]
Combined	6.2±0.7[b]	4.8±0.9	4.4±0.8[b]

The combined fold-increase was calculated by comparing 2% pO2 with insulin to the control group.

[a]Indicates a significant effect, $p<0.05$.

[b]For the combined treatment indicates a significant interaction ($p<0.05$) according to the ANOVA analysis, indicative of an interdependent effect. Three independent experiments were analyzed for UTS and modulus, and two independent experiments for collagen/cell

ANOVA, analysis of variance; UTS, ultimate tensile strength.

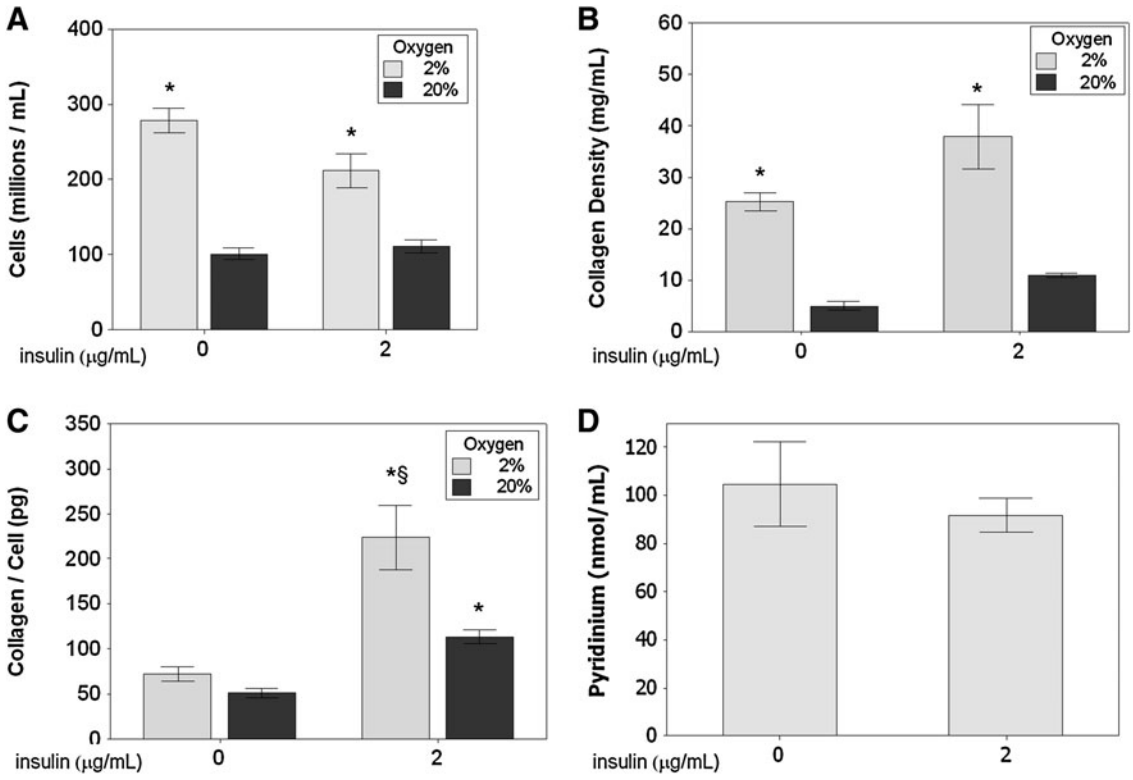

FIG. 3. Cell and protein density results for tissue constructs after 5 weeks of culture. **(A)** Cell density. Hypoxic culture (2% pO_2) resulted in an increase in the cell density. **(B)** Collagen density. Hypoxic culture resulted in a 4.5-fold increase in collagen density. **(C)** Per-cell collagen deposition. Insulin supplementation (2 μg/mL) resulted in a significant increase in collagen deposition, with an additional increase under hypoxic conditions. **(D)** Pyridinium density for hypoxic tissues. No difference was observed between insulin and noninsulin supplemented tissues. $n = 8$ for each cell and collagen density bar (two independent experiments); $n = 3$ for each pyridinium bar. $^*p < 0.05$ compared with control (20% pO_2, no insulin group). $^{\S}p < 0.05$ compared with all other groups.

Pyridinium cross-link density was measured by an EIA in constructs cultured in hypoxic conditions (2% pO_2) with and without insulin supplementation to evaluate collagen cross-link formation and its potential impact on mechanical properties. No difference was observed in the pyridinium cross-link concentration between the two groups, as shown in Figure 3D.

Histology

Histological analyses with Lillie's trichrome, as shown in Figure 4, provided a qualitative comparison to the cell and collagen density data that are shown in Figure 3. The highest cell and collagen densities were obtained by 2% pO_2 with insulin treatment and the darkest relative staining was observed in the same treatment group as shown in Figure 4A. Conversely, the lowest cell and collagen densities were measured in the 20% pO_2 without insulin group, which exhibited different staining compared with the other groups (Fig. 4D). Red staining with Lillie's trichrome is indicative of noncollagenous protein, which appeared more abundant in this case.

Western blots

Western blots were used to examine collagen production pathways in an effort to gain insight into potential explanations for the observation that the combined hypoxia and insulin treatment improved tissue mechanical properties. Blots for pAkt, tAkt, pERK, tERK, and procollagen P4H were examined by densitometry and normalized to the 20% pO_2 without insulin group. Figure 5 shows that there was an increase in the pAkt:tAkt ratio in the insulin-supplemented groups. This result was not affected by DO, indicating that Akt was activated in the presence of insulin regardless of ambient oxygen tension. Though Akt was found to be activated, the pERK:tERK ratio did not differ among the treatment groups. Levels of P4H were increased in the presence of insulin and two-way ANOVA further showed an interaction between pO_2 and insulin supplementation. In particular, the increased P4H induced by insulin supplementation was further increased in hypoxic culture.

Discussion

This study demonstrates that hypoxia with insulin supplementation can lead to increased collagen deposition that in turn yields greater strength and stiffness of tissue constructs made from nhDF-remodeled fibrin after 5 weeks of culture. Increased cell proliferation was also observed under hypoxic conditions, as previously reported for dermal fibroblasts on tissue culture plastic by Balin and Pratt.[36]

Further examination of these data (Figs. 2 and 3) revealed that hypoxia alone did not increase collagen deposition on a per-cell basis; however, hypoxia and insulin supplementation together yielded substantially greater collagen

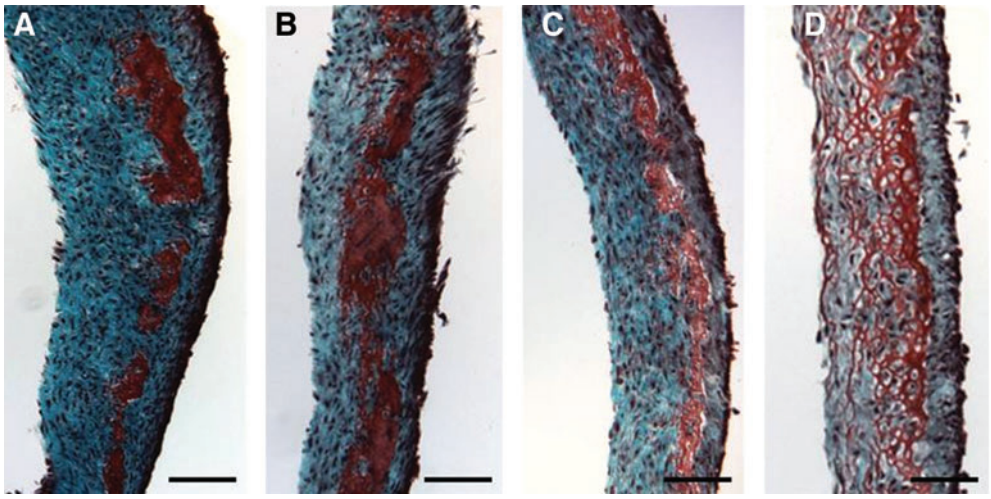

FIG. 4. Lillie's trichrome-stained sections of the fibrin-based tissue cultured under different treatment groups for 4 weeks. Collagen stains blue-green while noncollagenous proteins stain red. **(A)** 2% $pO_2$with 2 μg/mL insulin, **(B)** 2% pO_2 without insulin, **(C)** 20% pO_2 with insulin, and **(D)** 20% pO_2 without insulin. All sections were obtained from tissue cultured during a single experiment, fixed similarly, and sectioned to the same thickness. Scale bar = 200 μm. Color images available online at www.liebertonline.com/tea

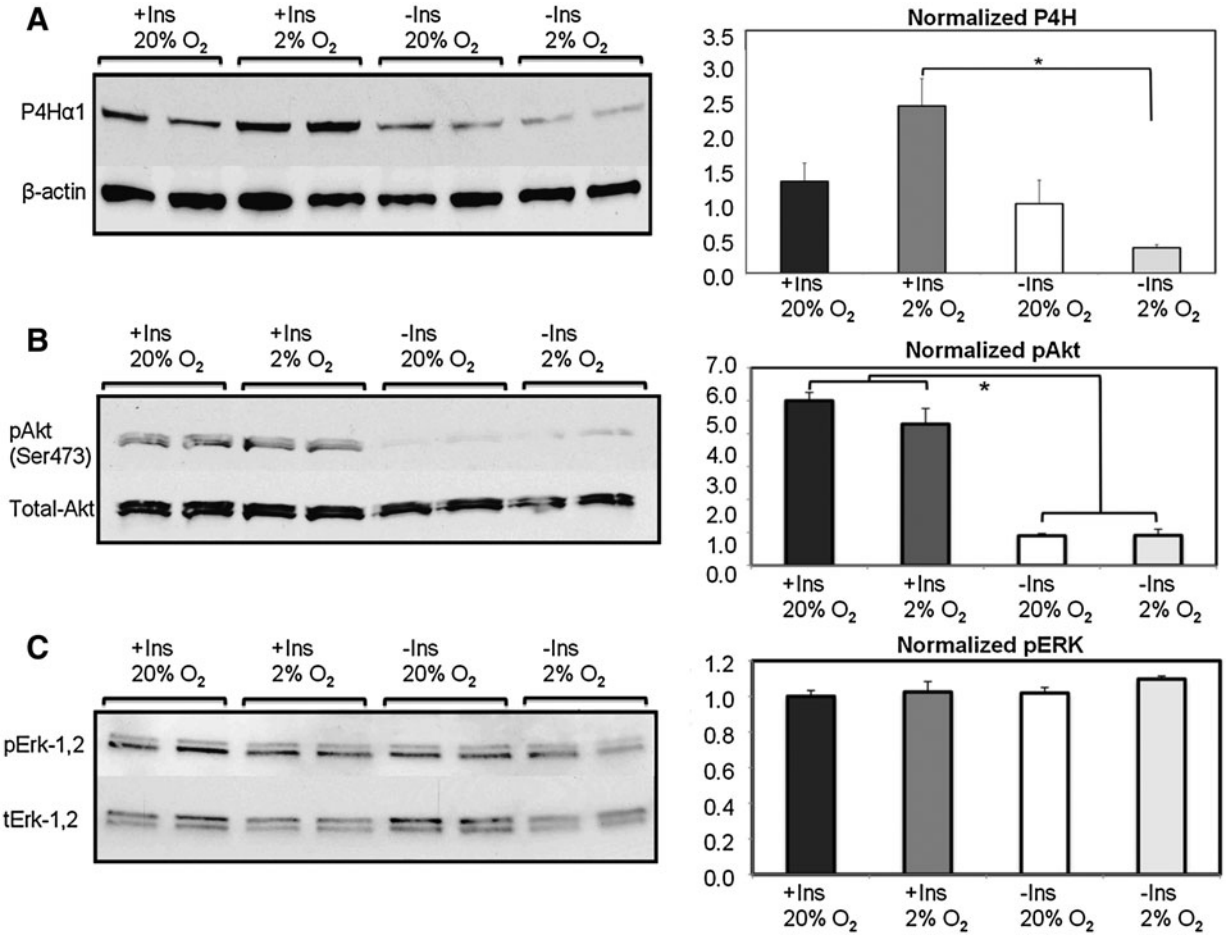

FIG. 5. Western blot analysis of signaling mechanisms implicated in hypoxic tissue development. The control group in each set is 20% pO_2 without insulin, which is normalized to a relative intensity of 1.0 (±SEM). **(A)** P4H, scaled to β-actin, was substantially elevated in the presence of insulin and 2% pO_2 compared with all other treatment groups. **(B)** Insulin supplementation led to increased Akt phosphorylation at serine-473. **(C)** ERK activation was unaffected by the treatment conditions evaluated. P4H, prolyl-4-hydroxylase; ERK, extracellular signal-regulated kinase. *$p < 0.05$.

deposition per cell. The effect of increased collagen density is also qualitatively apparent in Figure 4, whereby more intense collagen staining is shown among tissues of similar thickness. These results are consistent with previous studies demonstrating the impact of insulin supplementation on increased UTS, modulus, and collagen density.[8,14]

Since hypoxia and insulin could act to increase tissue and strength by means other than increased collagen density, additional experiments were performed to eliminate some alternatives. Constructs treated with sodium azide to kill the cells exhibited no difference in mechanical properties compared to nonazide treated samples, which indicates that there was no cellular contribution to the measured strength and stiffness. Sodium azide in the presence of protease inhibitors to kill cells was used for this assessment versus detergents to remove cells because detergents can cause loss of ECM components,[37] although we have found decellularization results in negligible change in tensile properties as well (data not shown). Furthermore, the density of pyridinium, a mature collagen cross-link,[38] was not different between insulin and noninsulin supplemented constructs cultured under hypoxic conditions. These measurements imply that an increase in deposited collagen and resultant increase in collagen density, induced by the combined treatment of hypoxia and insulin supplementation, largely explain the increase in strength and stiffness of the engineered tissue.

Preliminary investigations conducted at 5% pO_2 showed no increase in mechanical properties or collagen deposition (data not shown). Further experimentation was conducted using 2% pO_2, similar to work conducted by Falanga *et al.*,[18] which demonstrated increased collagen content with hDFs cultured at this pO_2. Given the low level of oxygen available, the theoretical DO profile was calculated to understand the minimum DO experienced by cells throughout the tissue. As shown in Figure 1, the DO profile for 2% pO_2 when cultured under static conditions is very near 0 nmol/mL throughout the tissue, with a minimum of 0.2 nmol/mL at the lumenal surface. Oxygen concentrations at this level cannot support aerobic respiration.[17] Static cultures subjected to 2% pO_2 resulted in unremodeled fibrin and cell death (data not shown). The mathematical model revealed that mixing the culture helps to maintain the profile above 2 nmol/mL throughout the tissue. Despite this low value (corresponding to 0.2% pO_2), the observation of increased collagen deposition at these oxygen tensions indicates it was sufficient to maintain the reactions involved in collagen posttranslational modifications requiring molecular oxygen, namely proline hydroxylation. Since the Michaelis–Menten parameters were obtained for fibroblasts in suspension, after trypsinization, the cells were stressed before testing and not in their normal elongated and adherent state. This could affect their OCR, as has been shown for chondrocytes,[39] and therefore the model predictions.

An interesting result of this study is the interdependent effects of the treatment groups on UTS and collagen deposited per cell (Table 1), which has not been previously shown. For these responses, the ANOVA indicated a statistically significant interaction term. These data suggest that hypoxia and insulin supplementation act in concert to promote increased collagen deposition and tensile strength and observed for samples exposed to both modes of stimulation. Inspection of tensile testing results for noninsulin supplemented samples would suggest that hypoxia alone had an effect; however, this result can be attributed to the increased cell density in these samples.

Balguid *et al.* conducted a comparable study using human saphenous vein cells, although the pO_2 was 7% rather than 2%.[14] Rectangular strips of tissue were constructed using a scaffold consisting of a porous degradable synthetic polymer and fibrin gel to deliver and retain cells within the pores. The authors found that 7% pO_2 yielded tissues with greater strength and stiffness; however, the magnitude of the effect was lower than reported here and the effect of insulin was not apparent. This could be due to cell type differences or the degradable polymer scaffold they used.

Western blotting was employed to examine the impact of hypoxia and insulin on collagen signaling pathways. One pathway of interest involves PI3K/Akt. Goldstein *et al.* demonstrated that both insulin and insulin-like growth factor-I (IGF-I) supplementation in lung fibroblast monolayers led to increased collagen mRNA via the IGF-I receptor,[40] consistent with binding of insulin to the IGF-1 receptor.[41] Gillery *et al.*[42] extended these results with IGF-I supplementation in 3D collagen and fibrin gels. One downstream effect of IGF-I activation is increased Akt phosporylation,[42,43] with pAkt being linked to increased collagen deposition in human dermal fibroblasts.[44] Western blots from this study (Fig. 5) show an increased pAkt:tAkt ratio with insulin supplementation with no effect due to pO_2. Further, ERK was found to remain largely unchanged with hypoxia and/or insulin supplementation. These findings together agree with separate literature studies evaluating the impact of IGF-I[45] or bleomycin supplementation[26] on PI3K/Akt and ERK activation. In the latter case, it was shown that observed increases in collagen production in lung fibroblasts were a response from activation of the PI3K-Akt pathway, not the ERK pathway. The results presented herein agree with these findings, as ERK phosphorylation did not differ between the treatment groups evaluated.

Posttranslational modification of procollagen by P4H was also of interest as proline hydroxylation in procollagen is critical to the stability and proper assembly of collagen fibers.[46] Horino *et al.* demonstrated that collagen deposition is accelerated by culturing lung fibroblasts in hypoxic conditions.[24] Their studies indicated that prolonged hypoxia (up to 9 days) resulted in no change of collagen mRNA levels, but increased levels of deposited collagen occurred due to increased levels of collagen P4H, which served to accelerate posttranslational modification. Takahashi *et al.* showed that the increased levels of P4H were directly due to hypoxia.[47] Herein, Western blot analysis indicated hypoxia led to substantially elevated P4H, but only in the presence of insulin supplementation, being nearly two-fold greater than that observed for the next highest treatment group (20% pO_2 with insulin). These data suggest an interdependence of insulin signaling and hypoxic conditions leading to increased P4H that subsequently improved the mechanical properties observed in these samples. The cause for differences reported here compared with Takahashi *et al.* are unclear, but could be due to the differences in cell type or 3D culture in remodeled fibrin compared with tissue culture plastic. Other biochemical pathways that could lead to increased collagen deposition involve decreased matrix metalloproteinase (MMP) degradation. However, several researchers have found that

MMP-1 (collagenase) is actually upregulated at the transcriptional and secretion levels in dermal fibroblasts when cultured under hypoxic conditions.[48–50] It was also found that tissue inhibitor of metalloproteinase-1 expression was not changed.[49] Thus, though increased collagen was deposited in the experiments presented here, there also exists the potential of increased turnover due to a simultaneous increase in collagen fibril assembly and degradation. Other hypoxia signaling mechanisms, such as production of hypoxia inducible factor and vascular endothelial growth factor have been reported[51,52] and may also be important in this system, including effects on collagen cross-linking and collagen synthesis.[49]

Conclusions

In this study, we examined the effect of insulin supplementation (2 μg/mL) and hypoxic culture (2% pO_2) on collagen deposition and mechanical properties of tubular tissue constructs made from nhDF-remodeled fibrin. The results presented here demonstrate that insulin-supplemented tissues cultured under hypoxic conditions exhibited increased collagen density, which served to increase the mechanical strength and stiffness three to four-fold over controls. Western blot analysis showed that the combined treatments increased Akt phosphorylation and P4H, temporally distinct factors promoting collagen transcription and posttranslational modification, respectively, consistent with the aforementioned effects of hypoxia and insulin supplementation. These findings highlight the potential of utilizing insulin supplementation and hypoxic culture to increase the mechanical strength and stiffness of fibrin-based engineered tissues.

Acknowledgments

The technical assistance of Naomi Ferguson and Ying Lung Lee is gratefully acknowledged. This work was supported by the National Institutes of Health (NHLBI R01 HL083880 to RTT) and 3M Company (JWB).

Disclosure Statement

No competing financial interests exist.

References

1. Lloyd-Jones, D., Adams, R.J., Brown, T.M., Carnethon, M., Dai, S., De Simone, G., *et al.* Heart disease and stroke statistics-2010 update a report from the American Heart Association. Circulation **121,** E46, 2010.
2. Konig, G., McAllister, T.N., Dusserre, N., Garrido, S.A., Iyican, C., Marini, A., *et al.* Mechanical properties of completely autologous human tissue engineered blood vessels compared to human saphenous vein and mammary artery. Biomaterials **30,** 1542, 2009.
3. Rashid, S.T., Fuller, B., Hamilton, G., and Seifalian, A.M. Tissue engineering of a hybrid bypass graft for coronary and lower limb bypass surgery. FASEB J **22,** 2084, 2008.
4. Tschoeke, B., Flanagan, T.C., Cornelissen, A., Koch, S., Roehl, A., Sriharwoko, M., *et al.* Development of a composite degradable/nondegradable tissue-engineered vascular graft. Artif Organs **32,** 800, 2008.
5. Barocas, V.H., and Tranquillo, R.T. An anisotropic biphasic theory of tissue-equivalent mechanics: the interplay among cell traction, fibrillar network deformation, fibril alignment, and cell contact guidance. J Biomech Eng **119,** 137, 1997.
6. Grassl, E.D., Oegema, T.R., and Tranquillo, R.T. Fibrin as an alternative biopolymer to type-I collagen for the fabrication of a media equivalent. J Biomed Mater Res **60,** 607, 2002.
7. Ahmed, T.A.E., Dare, E.V., and Hincke, M. Fibrin: a versatile scaffold for tissue engineering applications. Tissue Eng Part B-Rev **14,** 199, 2008.
8. Grassl, E.D., Oegema, T.R., and Tranquillo, R.T. A fibrin-based arterial media equivalent. J Biomed Mater Res **66A,** 550, 2003.
9. Ahmann, K.A., Weinbaum, J.S., Johnson, S.L., and Tranquillo, R.T. Fibrin degradation enhances vascular smooth muscle cell proliferation and matrix deposition in fibrin-based tissue constructs fabricated in vitro. Tissue Eng Part A **16,** 3261, 2010.
10. Syedain, Z.H., Weinberg, J.S., and Tranquillo, R.T. Cyclic distension of fibrin-based tissue constructs: evidence of adaptation during growth of engineered connective tissue. Proc Natl Acad Sci U S A **105,** 6537, 2008.
11. Syedain, Z.H., and Tranquillo, R.T. Controlled cyclic stretch bioreactor for tissue-engineered heart valves. Biomaterials **30,** 4078, 2009.
12. Syedain, Z.H., Meier, L.A., Bjork, J.W., Lee, A., and Tranquillo, R.T. Implantable arterial grafts from human fibroblasts and fibrin using a multi-graft pulsed flow-stretch bioreactor with noninvasive strength monitoring. Biomaterials **32,** 714, 2011.
13. Long, J.L., and Tranquillo, R.T. Elastic fiber production in cardiovascular tissue-equivalents. Matrix Biol **22,** 339, 2003.
14. Balguid, A., Mol, A., van Vlimmeren, M.A.A., Baaijens, F.P.T., and Bouten, C.V.C. Hypoxia induces near-native mechanical properties in engineered heart valve tissue. Circulation **119,** 290, 2009.
15. Ray, J.B., Arab, S., Deng, Y., Liu, P., Penn, L., Courtman, D.W., *et al.* Oxygen regulation of arterial smooth muscle cell proliferation and survival. Am J Physiol Heart Circ Physiol **294,** H839, 2008.
16. Bjornheden, T., Evaldsson, M., and Wiklund, O. A method for the assessment of hypoxia in the arterial wall, with potential application *in vivo*. Arterioscler Thromb Vasc Biol **16,** 178, 1996.
17. Leach, R.M., and Treacher, D.F. ABC of oxygen—Oxygen transport-2. Tissue hypoxia. Br Med J **317,** 1370, 1998.
18. Falanga, V., Qian, S.W., Danielpour, D., Katz, M.H., Roberts, A.B., and Sporn, M.B. Hypoxia up-regulates the synthesis of TGF-Beta-1 by human dermal fibroblasts. J Investig Dermatol **97,** 634, 1991.
19. Falanga, V., Zhou, L., and Yufit, T. Low oxygen tension stimulates collagen synthesis and COL1A1 transcription through the action of TGF-beta 1. J Cell Physiol **191,** 42, 2002.
20. Malda, J., Martens, D.E., Tramper, J., van Blitterswijk, C.A., and Riesle, J. Cartilage tissue engineering: controversy in the effect of oxygen. Crit Rev Biotechnol **23,** 175, 2003.
21. Heywood, H.K., and Lee, D.A. Low oxygen reduces the modulation to an oxidative phenotype in monolayer-expaned chondrocytes. J Cell Physiol **222,** 248, 2010.
22. Lewis, M.C., MacArthur, B.D., Malda, J., Pettet, G., and Please, C.P. Heterogeneous proliferation within engineered cartilaginous tissue: the role of oxygen tension. Biotechnol Bioeng **91,** 607, 2005.

23. Sander, E.A., and Nauman, E.A. Effects of reduced oxygen and glucose levels on ocular cells *in vitro*: implications for tissue models. Cells Tissues Organs **191,** 141, 2010.
24. Horino, Y., Takahashi, S., Miura, T., and Takahashi, Y. Prolonged hypoxia accelerates the posttranscriptional process of collagen synthesis in cultured fibroblasts. Life Sci **71,** 3031, 2002.
25. Neidert, M.R., Lee, E.S., Oegema, T.R., and Tranquillo, R.T. Enhanced fibrin remodeling *in vitro* with TGF-beta 1, insulin and plasmin for improved tissue-equivalents. Biomaterials **23,** 3717, 2002.
26. Lu, Y.J., Azad, N., Wang, L.Y., Iyer, A.K.V., Castranova, V., Jiang, B.H., *et al.* Phosphatidylinositol-3-kinase/Akt regulates bleomycin-induced fibroblast proliferation and collagen production. Am J Respir Cell Mol Biol **42,** 432, 2010.
27. Papakrivopoulou, J., Lindahl, G.E., Bishop, J.E., and Laurent, G.J. Differential roles of extracellular signal-regulated kinase 1/2 and p38(MAPK) in mechanical load-induced procollagen alpha(1)(I) gene expression in cardiac fibroblasts. Cardiovasc Res **61,** 736, 2004.
28. Tuan, T.L., and Grinnell, F. Fibronectin and fibrinolysis are not required for fibrin gel contraction by human-skin fibroblasts. J Cell Physiol **140,** 577, 1989.
29. Bjork, J.W., and Tranquillo, R.T. Transmural flow bioreactor for vascular tissue engineering. Biotechnol Bioeng **104,** 1197, 2009.
30. Papas, K.K., Pisania, A., Wu, H., Weir, G.C., and Colton, C.K. A stirred microchamber for oxygen consumption rate measurements with pancreatic islets. Biotechnol Bioeng **98,** 1071, 2007.
31. Radisic, M., Malda, J., Epping, E., Geng, W.L., Langer, R., and Vunjak-Novakovic, G. Oxygen gradients correlate with cell density and cell viability in engineered cardiac tissue. Biotechnol Bioeng **93,** 332, 2006.
32. Sengers, B.G., van Donkelaar, C.C., Oomens, C.W.J., and Baaijens, F.P.T. Computational study of culture conditions and nutrient supply in cartilage tissue engineering. Biotechnol Prog **21,** 1252, 2005.
33. Starcher, B. A ninhydrin-based assay to quantitate the total protein content of tissue samples. Anal Biochem **292,** 125, 2001.
34. Stegemann, H., and Stalder, K. Determination of hydroxyproline. Clin Chim Acta **18,** 267, 1967.
35. Kim, Y.J., Sah, R.L.Y., Doong, J.Y.H., and Grodzinsky, A.J. Fluorometric assay of DNA in cartilage explants using Hoechst-33528. Anal Biochem **174,** 168, 1988.
36. Balin, A., and Pratt, L. Oxygen Modulates The growth of skin fibroblasts. In Vitro Cell Dev Biol Anim **38,** 305, 2002.
37. Crapo, P.M., Gilbert, T.W., and Badylak, S.F. An overview of tissue and whole organ decellularization processes. Biomaterials **32,** 3233, 2011.
38. Eyre, D.R., Paz, M.A., and Gallop, P.M. Cross-linking in collagen and elastin. Annu Rev Biochem **53,** 717, 1984.
39. Guaccio, A., Borselli, C., Oliviero, O., and Netti, P. Oxygen consumption of chondrocytes in agarose and collagen gels: a comparative analysis. Biomaterials **29,** 1484, 2008.
40. Krupsky, M., Fine, A., Kuang, P.P., Berk, J.L., and Goldstein, R.H. Regulation of type I collagen production by insulin and transforming growth factor-beta in human lung fibroblasts. Connect Tissue Res **34,** 53, 1996.
41. Goldstein, R.H., Poliks, C.F., Pilch, P.F., Smith, B.D., and Fine, A. Stimulation of collagen formation by insulin and insulin-like growth factor-I in cultures of human-lung fibroblasts. Endocrinology **124,** 964, 1989.
42. Gillery, P., Leperre, A., Maquart, F.X., and Borel, J.P. Insulin-like growth factor-I (IGF-I) stimulates protein-synthesis and collagen gene-expression in monolayer and lattice cultures of fibroblasts. J Cell Physiol **152,** 389, 1992.
43. Yin, W.H., Park, J.I., and Loeser, R.F. Oxidative stress inhibits insulin-like growth factor-i induction of chondrocyte proteoglycan synthesis through differential regulation of phosphatidylinositol 3-kinase-Akt and MEK-ERK MAPK signaling pathways. J Biol Chem **284,** 31972, 2009.
44. Bujor, A.M., Pannu, J., Bu, S., Smith, E.A., Muise-Helmericks, R.C., and Trojanowska, M. Akt blockade downregulates collagen and upregulates MMP1 in human dermal fibroblasts. J Investig Dermatol **128,** 1906, 2008.
45. Chetty, A., Cao, G.J., and Nielsen, H.C. Insulin-like growth factor-I signaling mechanisms, type I collagen and alpha smooth muscle actin in human fetal lung fibroblasts. Pediatr Res **60,** 389, 2006.
46. Myllyharju, J. Prolyl 4-hydroxylases, the key enzymes of collagen biosynthesis. Matrix Biol **22,** 15, 2003.
47. Takahashi, Y., Takahashi, S., Shiga, Y., Yoshimi, T., and Miura, T. Hypoxic induction of prolyl 4-hydroxylase alpha(I) in cultured cells. J Biol Chem **275,** 14139, 2000.
48. Ahn, J.K., Koh, E.M., Cha, H.S., Lee, Y.S., Kim, J., Bae, E.K., *et al.* Role of hypoxia-inducible factor-1 alpha in hypoxia-induced expressions of IL-8, MMP-1 and MMP-3 in rheumatoid fibroblast-like synoviocytes. Rheumatology **47,** 834, 2008.
49. Kan, C., Abe, M., Yamanaka, M., and Ishikawa, O. Hypoxia-induced increase of matrix metalloproteinase-1 synthesis is not restored by reoxygenation in a three-dimensional culture of human dermal fibroblasts. J Dermatol Sci **32,** 75, 2003.
50. Karakiulakis, G., Papakonstantinou, E., Aletras, A.J., Tamm, M., and Roth, M. Cell type-specific effect of hypoxia and platelet-derived growth factor-BB on extracellular matrix turnover and its consequences for lung remodeling. J Biol Chem **282,** 908, 2007.
51. van Vlimmeren, M.A.A., Driessen-Mol, A., van den Broek, M., Bouten, C.V.C., and Baaijens, F.P.T. Controlling matrix formation and cross-linking by hypoxia in cardiovascular tissue engineering. J Appl Physiol **109,** 1483, 2010.
52. Ke, Q.D., and Costa, M. Hypoxia-inducible factor-1 (HIF-1). Mol Pharmacol **70,** 1469, 2006.

Address correspondence to:
Robert T. Tranquillo, Ph.D.
Department of Chemical Engineering and Materials Science
University of Minnesota
151 Amundson Hall
421 Washington Ave. SE
Minneapolis, MN 55455

E-mail: tranquillo@umn.edu

Received: January 10, 2011
Accepted: October 18, 2011
Online Publication Date: December 2, 2011

(*Appendix follows* →)

Appendix

The mathematical model for static culture of the tubular constructs was developed to understand the severity of dissolved oxygen (DO) gradients without any mixing during incubation in a culture dish. The general species balance equation for DO in tissue is shown in Equation 1:

$$\frac{\partial C_{O_2}}{\partial t} + \underline{v} \cdot \nabla C_{O_2} = D_{O_2,t}\, \nabla^2 C_{O_2} - R_{O_2} \tag{1}$$

where $D_{O_2,t}$ is the diffusivity of oxygen in tissue, C_{O_2} is the DO concentration, $\underline{v}$ is the velocity vector, and R_{O_2} is the oxygen consumption rate. Simplifying for steady-state, diffusion-only DO transport, and assuming Michaelis–Menten kinetics for oxygen consumption within the tissue yields Equation 2:

$$D_{O_2,t}\nabla^2 C_{O_2} = \rho_{cell}\frac{V_{O_2\max} C_{O_2}}{K_m + C_{O_2}} \tag{2}$$

where $\rho\ cell$ is the cell density, and $V_{O_2\max}$ and K_m are the Michaelis–Menten parameters. The system consisted of two subdomains–the tissue and the culture medium surrounding the tissue as illustrated in Figure 1B. Equation 2 was solved with the boundary conditions shown in Equations 3–5:

$$C_{O_2}\Big|_{y=0} = \alpha P_\infty \tag{3}$$

$$\frac{\partial C_{O_2}}{\partial r}\Big|_{r=R_i} = 0 \tag{4}$$

$$J_{O_2,tissue}\Big|_{r=R_o} = J_{O_2,fluid}\Big|_{r=R_o} \tag{5}$$

where α is the Bunsen solubility coefficient for oxygen in 37°C cell culture medium,[29] P_∞ is the surrounding air oxygen tension, and J_{O2} represents the oxygen flux. Equation 4 represents a zero flux boundary at the construct lumen since culture is on a glass mandrel, assumed impermeable to O_2. Similarly, a zero flux boundary was prescribed at $x=0$, as shown in Figure 1B.

A well-mixed assumption was used to simplify the model for mixed cultures. In this case, the concentration throughout the liquid domain was assumed to be equal to the value provided by Equation 3. Thus, the boundary conditions for the well-mixed case were simplified to:

$$C_{O_2}\Big|_{r=R_o} = \alpha\ P_\infty \tag{6}$$

$$\frac{\partial C_{O_2}}{\partial r}\Big|_{r=R_i} = 0 \tag{7}$$

These equations were then input to COMSOL and solved to provide the tissue DO concentration profiles illustrated in Figure 1C.